 FDMP, vol.9, no.1, pp.77-89, 2013

Experimental Investigation of Internal Channel Cooling Via Jet Impingement

Emad Elnajjar[1], **Mohammad O. Hamdan, Yousef Haik**

Abstract: In this paper, two heat transfer configurations (central-jet and side-jet) of jet impinging on a semicircular surface are experimentally studied. The internal channel is formed using flat insulated wall and a semi-circular surface using a curved flexible heater with a uniform heat flux. A set of experiments have been performed for the purpose of assessing the heat augmentation and pressure drop between the two jet configurations. The measurements include the inlet and outlet flow temperatures using thermocouples, the temperature map of the flexible heater using thermal infra-red camera, the flow rates using rotary meter and pressure drop using pressure transducer. The study covers a jet flow Reynolds Numbers of 500 to 5000. The heat transfer is estimated by calculating the average and local heat transfer coefficient under constant wall heat flux condition and the pumping pressure is estimated by measuring the pressure drop between the inlet and outlet. The results indicate that central-jet impingement shows a 50% improvement in heat transfer with minimal difference in pumping pressure compared to the side-jet for the same range of Reynolds numbers.

Keywords: Thermography, internal channel cooling, side-jet entry, central-jet entry

1 Introduction

Many engineering applications are utilizing jet impingement for cooling, drying, and enhancing heat transfer. The jet cooling applications include internal channel cooling, bearing cooling, electronics cooling, vehicle windshield deicing/defogging, drying of paper, and glass tempering. There are many applications that demand enhancing and optimizing the heat transfer due to jet impingement. The jet impingement is used widely in the industry to achieve and enhance internal channel cooling. The internal channel cooling can be achieved by different augmentation techniques such as jet impingement [Vijay (2002)], porous inserts [Hamdan and

[1] Mechanical Engineering Department, United Arab Emirates University, Al-Ain, Abu Dhabi, UAE

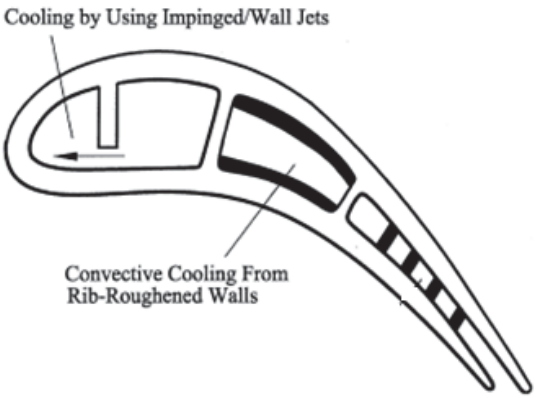

Figure 1: Gas Turbine Blade cross section view with the wall/impinged jet cooling in the leading-edge circuit.

Al-Nimr (2009)], roughness elements, ribs [Dutta and Hossain (2005)], or pin fins. Scientists are manipulate flow pattern via changing jet locations in order to enhance heat transfer, reduce pressure drop, and minimize stagnation region. The internal channel cooling utilizing jet flow has been used for cooling the leading edge in gas turbine blade [Hwang and Cheng (2001); Je-Chin (2004)]. A cross sectional view of the turbine blade is shown in Fig. 1 where a side-entry jets is introduced tangentially into the leading-edge cooling channel traverse one principal wall, then directly impinge on the other principal wall, and finally purge in the chord direction from the blade tip. For turbine blade, the temperature gradient is one of the mechanisms that cause crack and material loss; hence several numerical and experimental studies have been conducted in order to provide better cooling with a small temperature gradient. Hwang and Cheng (2001) investigated experimentally the effect of enhancing the internal channel cooling by impinging the cooling fluid using swirl chamber. Hwang and Cheng showed that the heat transfer increases with the jet Reynolds. Previous studies showed that the heat transfer of impinged jet on a curved surface is increased by 20% comparing to an impinging jet over a flat surface. The mechanism of enhancing the heat transfer of this configuration is not fairly understood, and this enhancement is believed to be due to the complexity of the flow structures and that the curvature of the surface adds to the developed flow. Flow structures such as the turbulence boundary layer which is developed on the curved surface, the interaction of jet flow entrainment and the developed shear layer, the impinged stagnation region and the generated cyclone at the center of the inlet/outlet jet flow contribute to the heat transfer performance.

A few studies have been conducted addressing the heat transfer of impinging jet on a curved surface. Kayansayan and Kucuka (2001) experimentally studied the cooling effect of a slot jet impinged over an isothermal semi-cylinder concave channel. Their study covered a range of normalized jet width to impinging distance from the jet exit (ranging from 2.2 to 4.2) and a range of jet Reynolds numbers from 200 to 11,000. Eren, Yesilata, and Celik (2007) performed an experimental study investigating the heat transfer augmentation of a jet flow on unconfined convex and slightly convex constant heat flux surfaces. The study carried out for a range of Reynolds number from 8617 to 15415 for a constant jet to impingement surface distance of 8 cm.

Thomann (1968) investigated the effect of the curvature on jet impingement cooling. He found that due to the curvature, the centripetal forces generate flow instability "known as Taylor-Gortler instability", which produces a double vortex that enhances the flow mixing, that in turn leads to heat transfer augmentation.

Choia, Yooa, Yanga, Leea, and Sohna (2000) experimentally investigated the cooling effect of impinging slot-jet on the center of unconfined semi-circular concave surface. The study considered the variation of different parameters including: Reynolds numbers and nozzle-to-surface distances. The study reported the heat transfer, and field flow turbulence measurements. Their results were considered a bench mark and had been used for model validation for cases with similar geometry.

Sharif and Mothe (2010) ran a numerically parametric study of slot-jet impingement on unconfined constant flux cylindrical surface. The numerical simulation was carried out using the commercial software Fluent 6.3, using RNG k-turbulence model with two-layer near wall treatment and the simulated geometry was chosen similar to the one investigated by Choia, Yooa, Yanga, Leea, and Sohna (2000). The study covered a range of jet Reynolds number from 2000-12,000, a concave surface diameter to slot jet width of 30 and a range of distance of impingement surface from the jet exit to slot-jet width of 3, 9 and 12. Their results showed that the jet exit Reynolds number and the surface curvature have a significant effect on the heat transfer process. A Nusselt number correlation as function of the studied parameters was developed.

Hamdan, Elnajjar, and Haik (2011) investigated experimentally and numerically the heat transfer augmentation from a semicircular heated surface due to confined slot-jet impingement for different Reynolds numbers. The single enclosed jet is designed to strike the curved surface side and to create a single cyclone inside the internal semicircular channel to promote the heat transfer at different jet Reynolds numbers. Three turbulence models, namely, the standard $k-\varepsilon$, $k-\omega$ and the Reynolds stress model (RSM) have been investigated and by comparing Nusselt

number and normalized pressure drop distribution against the experimental data, helping ascertain on the relative merits of the adopted models. The computational fluid dynamics results show that the RSM turbulent model reasonably forecast the experimental data.

In the present work a comparison experimental study between two impinged jet flow configurations on a constant heat flux curved channel is carried out. The first geometry is a central-jet flow where the inlet jet flow is located at the center of the flat side of the channel. Whereas the second geometry is the side-side-jet jet where the inlet jet flow is located at one side of the flat side of the channel. The study covers a range of inlet jet Reynolds numbers from 500 to 5,000. The average Nusselt number and drag coefficient are used as a tool for the performance comparison between the two proposed configurations.

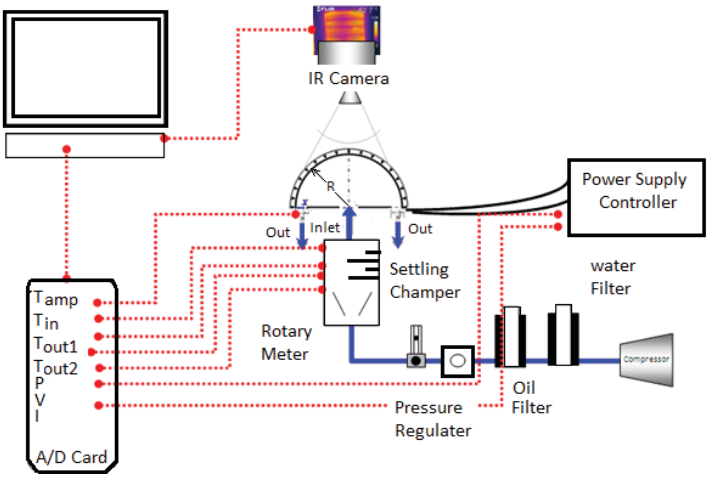

Figure 2: An experimental apparatus setup with an indication of main experimental data collected.

2 Experimental apparatus and procedure

The experimental setup for the heat transfer measurement inside the semi-circular bend is illustrated in Fig. 2. The impinged flow is air and it is introduced by a compressor, the air flow is regulated using a pressure regulator and a needle valve Type AR1500. The air flow is filtered to get rid of any oil droplet, dust and water mist from the compressed air lines. A carefully designed settling chamber is used to provide a uniform non-pulsating flow to the test setup. The air flow rate is measured

using a flow rotary meter Omega type FL-3607G with accuracy of $\pm 2\%$. A flexible tape heater with 10 *mm* width is used to form the semi-circular concave surface with 100 *mm* diameter and is supported by a semi-circular support at the edge. During the measurement of heat transfer coefficients, the surface is directly heated by applying an electric current through a flexible rubber heater that has a thickness of 0.4 *mm*. The heat flux applied on the surface is controlled by changing output voltage and determined by measuring the electrical current and the voltage drop, using a high accuracy Agilent HP 34401A digital multi meter type HP 2300 with accuracy of $\pm 0.0001V$.

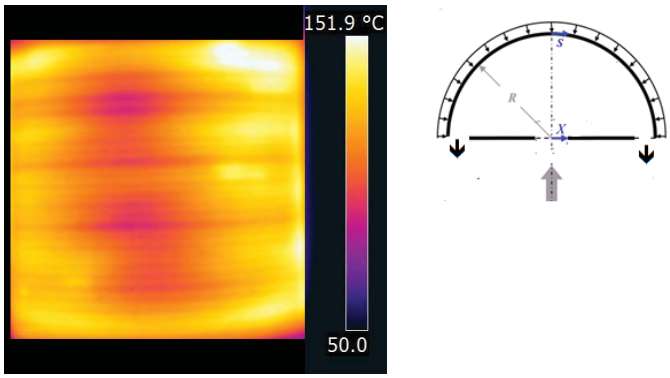

a) Central-jet Flow

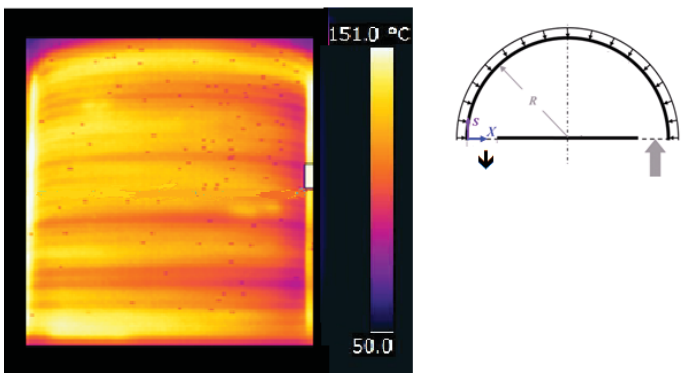

b) Side-Jet Flow

Figure 3: A thermography top view of the curved surface heater at $Re_{jet} = 1225$ and heat flux of $2048W/m^2$ (a) Schematic of the central-jet flow configuration with thermal map of the curved surface (b) Schematic of the side-jet flow configuration with thermal map of the curved surface.

The jet inlet pressure is measured using pressure transducer model 407910 From EXTECH instrument with an accuracy of 0.1 Pa and the jet inlet temperature is measured using K type thermocouple with an accuracy of 0.3 degree. The outlet flow is opened to the atmosphere and the outlet temperature is measured using the K-type thermocouple. The thermocouples are calibrated and compared with respect to the boiling water state. The local temperature distribution is measured using an infrared camera FLIR which provides an image of the back side of the heater as shown in Figure 3, the thermal temperature mapping is calibrated against thermocouple array over a curved surface simulating the used curved surface prior to experiment. The Reynolds number is calculated based on the hydrodynamic diameter of the inlet-jet which is 1.18 cm. For simplicity to handle the test setup, the width of the side-jet is selected to be 1 cm while the depth of the jet is selected to be 10 cm which matches the heater width. The temperature map is reported using infra-red camera and the temperature profile is reported in the middle of the cross section (section A-A) of the channel to minimize the effect of the side wall. The camera's settings and range are optimized to suit our case and the material of a flexible rubber surface heater. It is worth mentioning that the accuracy of the used instrumentation in the setup are $0.3^{\circ}C$, $0.1Pa$ and $0.5^{\circ}C$ for the thermocouples, the pressure transducer, flow rate and the infra-red camera, respectively. The uncertainty analysis was performed on the experimental measurements, where the calculated Nusselt number uncertainty was about $\pm 0.15\%$, while the average calculated drag coefficient uncertainty about $\pm 2.0\%$.

The local Nusselt number is calculated by:

$$Nu = \frac{q''}{T_s - T_{in}} \left(\frac{D_h}{k_f} \right) \tag{1}$$

while average Nusselt number is calculated by:

$$Nu_{avg} = \frac{q''}{(T_{s,avg} - T_{in})} \left(\frac{D_h}{k_f} \right) \tag{2}$$

The average drag coefficient is calculated by:

$$C_{D,avg} \frac{P_{in} - P_{out}}{1/2 \rho U^2} \tag{3}$$

The Reynolds Number is defined using the jet inlet hydrolic diameter as:

$$Re = \frac{\rho U D_h}{\mu} \tag{4}$$

3 Results and Discussion

Figure 3 shows the thermal map images of the top side of the curved surfaces for both configurations: central and side-jet flow. The surface is heated with a constant wall heat flux of 3183 W/m^2, for an inlet jet Reynolds number of 3570. The temperature mapping of the surface, as anticipated, shows a lower temperature region along the entrance of the jet flow at the middle of the channel for the central-jet case, roughly around an average of 100°C as shown in figure 3a, and a lower temperature mapping at the right side along the entrance region for the side-jet flow case, about an average temperature of 102°C as shown in figure 3b. An increased temperature toward the flow exit can be observed at each side of the central-jet channel and at the left side of the side-jet channel, around an average temperature of 130°C and 135°C respectively . This behavior is expected where the temperature of the heated surface is coldest near the jet entrance, the boundary layer thickness is the thinnest and the thermal resistance is smallest compared to the conditions at the channel outlet. Hence, at this region, the convective heat transfer is the highest. The flow gets hotter along the curvature of the surface as the air flow moves toward the channel jet outlet. Along the surface curvature from the jet inlet, the boundary layer thickness grows and reduces the convective heat coefficient.

For experiment validation and building a confident level on the experiment's results, an average Nusselt number for the central-Jet case as function of different Reynolds numbers is compared to an earlier work conducted by Sharif and Mothe (2010), as shown in Figure 4. The present experimental results had a satisfactory agreement with Sharif's empirical correlation.

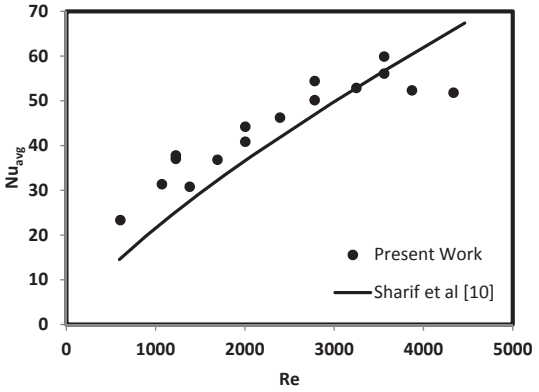

Figure 4: The variation of average Nusselt number versus Reynolds number for the central-Jet case. Comparing the present work to Sharif and Mothe (2010) correlation model.

The local dimensionless temperature defined as $(\theta = T/T_{in})$ along the normalized surface curvature distance defined as $(S = s/d)$, for the inlet jet Reynolds number of 3570, is shown in figure 5. The lowest local wall temperature is achieved at the region where the jet flow strikes the wall, which indicates the high local convective heat transfer coefficient. This behavior was observed for all used Reynolds numbers. On an average, for the same constant wall heat flux, the central-jet flow configuration case shows more than 10% reduction in the local wall temperature when compared to the side-jet configuration case.

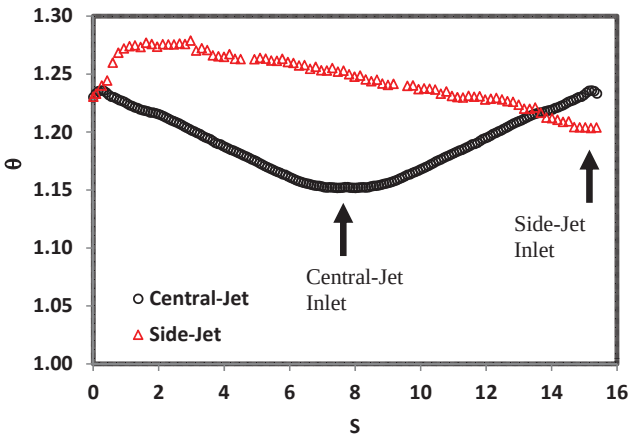

Figure 5: The local normalized temperature of the curved surface obtained at section A-A in figure 4, $Re_{jet} = 3570$ and heat flux of $3183 W/m^2$.

Figure 6 reports the local Nusselt number as a function of the normalized surface curvature distance, for the experimental of both channel configurations. For the central-jet case, at the region of the jet impingement on the center of the curved surface two hydraulic boundary layers, start to developed and grow at each side of the impingement point, due to the air entrainment. In a similar fashion two thermal boundary layers developed at each side. At the region of impingement, where the boundary layer is very thin, a high temperature gradient is anticipated, and as a consequence, a region of low thermal resistance and high local Nusselt number will be formed, Sharif and Mothe (2010) noticed similar behavior. A similar argument can be made for the side-jet configuration case where the hydraulic and thermal boundary layers are developed at the point of jet impingement at the entrance at the right side, where it will grow toward the left hand side of the channel configuration at the outlet side. Higher temperature gradients and higher local Nussselt

numbers are achieved at the jet impingement regions next to the jet inlet side. By comparing the local Nusselt number for both jet configuration at the inlet region, a 60% increase in local Nusselt number is attained for the central-jet over the side-Jet configuration case.

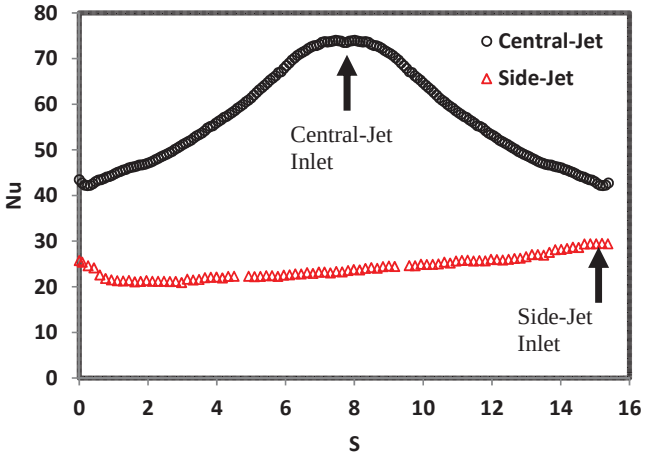

Figure 6: The local Nusselt number for the curved wall at $Re_{jet} = 3570$.

The variation of the average Nusselt number as a function of different inlet jet Reynolds numbers is shown in figure 7 for the central- and the side-jet channel flows configuration. The results suggest that the average Nusselt number increases almost linearly with jet Reynolds number for both cases. The witnessed behavior is expected, since, as Reynolds numbers increases, a smaller boundary layer thickness and higher temperature gradient are predicted and as a consequence a higher Nussult number is anticipated. A 50-60% increase of the average Nusselt number for the central-jet over the side-jet flow has been observed by the results. This suggests that for the same Reynolds number, the central-jet flow channel configuration provides a more efficient cooling configuration when compared to the side-jet flow channel, which is demonstrated for the current channel radius to jet ratio. This cannot be generalized to all ratios between the semi-circular diameters to the jet diameter due to the fact that, as the semi-circular diameter to jet diameter ratio decreases, it is expected that centrifugal force would have a more pronounced effect on the heat transfer.

The variation of the average drag coefficient as function of different inlet jet Reynolds number is shown in figure 8. The results suggest that the pressure drop in both jet channel flow configurations is the same as for all Reynolds numbers, in other words,

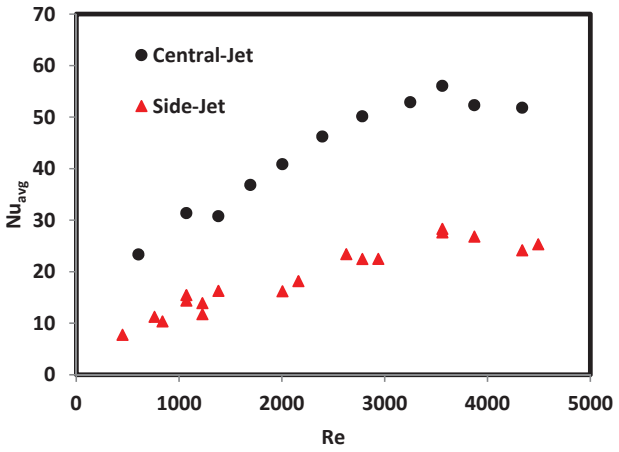

Figure 7: The variation of average Nusselt number versus Reynolds number for jet flow impinged on the curved heated surface.

for the same pumping pressure requirements, the two different configurations have no effect. This finding is true for a semi-circular channel with a radius five times the size of the jet width.

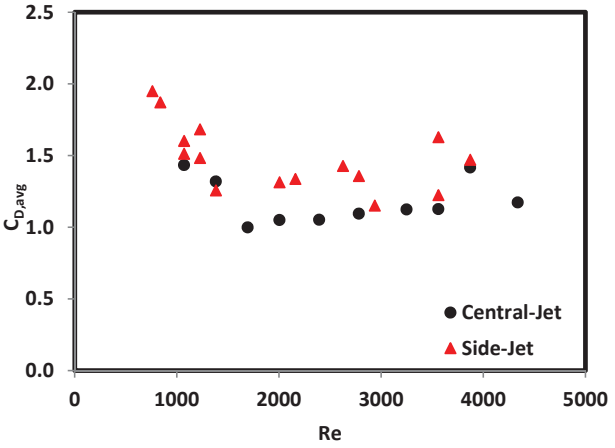

Figure 8: The variation of average drag coefficient versus Reynolds number for jet flow impinged on the curved heated surface.

4 Conclusions

This paper reports the effects of two configurations of jet impinging flow on the heat transfer augmentation and pumping pressure inside internal channel with a curved heated surface. In the first configuration the jet is impinged at the center of the channel and in the second configuration the jet is impinged at the side of the channel. The main observations are that both configurations experience an increase in the average Nusselt number as Reynolds number increases. The local Nusselt number at the inlet region of the central-jet case is higher than the side-jet case by an order of 60%. The average Nusselt number of the central-jet case is higher than the side-jet case by an order of 50%, and the two channel configurations have no noticeable different on the pumping pressure requirements for the same flow.

Acknowledgement: The authors would like to acknowledge the support provided by the United Arab Emirates University. This work was financially supported by the Research Affairs at the university under a contract no. 01-05-7-11/09.

References

Choia, M.; Yooa, H. S.; Yanga, G.; Leea, J. S.; Sohna, D. K. (2000): Measurements of impinging jet flow and heat transfer on a semi-circular concave surface. *International Journal of Heat and Mass Transfer*, vol. 43, pp. 1811–1822.

Dutta, P.; Hossain, A. (2005): Internal cooling augmentation in rectangular channel using two inclined baffles. *International Journal of Heat and Fluid Flow*, vol. 26, pp. 223–232.

Eren, H.; Yesilata, B.; Celik, N. (2007): Nonlinear flow and heat transfer dynamics of a slot jet impinging on a slightly-curved surfaces. *Applied Thermal Engineering*, vol. 27, pp. 2600–2608.

Hamdan, M.; Al-Nimr, M. A. (2009): Thermal augmentation in internal cooling passage by converting impingement jet to induced swirl flow. In *Proceedings 6th International Conference on Computational Heat and Mass Transfer*, pp. 257–262.

Hamdan, M. O.; Elnajjar, E.; Haik, Y. (2011): Measurement and modeling of confined jet discharged tangentially on a concave semicylindrical hot surface. *J. Heat Transfer*, vol. 133, no. 12, pp. 122203 (7 pages).

Hwang, J. J.; Cheng, C. S. (2001): Impingement cooling in triangular ducts using an array of side-entry wall jets. *International Journal of Heat and Mass Transfer*, vol. 44, pp. 1053–1063.

Je-Chin, H. (2004): Recent studies in turbine blade cooling. *International Journal of Rotating Machinery*, vol. 10, no. 6, pp. 443–457.

Kayansayan, N.; Kucuka, S. (2001): Impingement cooling of a semi-cylindrical concave channel by confined slot-air-jet. *Experimental Thermal and Fluid Science*, vol. 25, pp. 383–396.

Sharif, M. A. R.; Mothe, K. K. (2010): Parametric study of turbulent slot-jet impingement heat transfer from concave cylindrical surfaces. *International Journal of Thermal Sciences*, vol. 49, pp. 428–442.

Thomann, H. (1968): Effect of streamwise wall curvature on heat transfer in a turbulent boundary layer. *Journal of Fluid Mechanics*, vol. 33, pp. 283–292.

Vijay, K. G. (2002): Heat transfer research on gas turbine airfoils at nasa grc. *International Journal of Heat and Fluid Flow*, vol. 23, pp. 109–136.

Appendix A: Nomenclature

A	curved surface area, m^2
c	specific heat capacity, $kJ/kg.K$
d	jet inlet width, m
$C_{D,avg}$	Average drag coefficient,
D_h	jet inlet hydrolic diameter, $4Ld/(2L+2d)$
h	heat transfer coefficient, $h = q_{in}/(A\Delta T_{LM}), W/m^2.K$
$\bar{h}$	average heat transfer coefficient, $\bar{h} = q_{in}/(A\Delta T_{LM,avg}), W/m^2.K$
k_f	thermal conductivity of the fluid, $W/m.K$
L	jet inlet length, m
$\dot{m}$	mass flow rate, kg/s
Nu	local Nusselt number.
Nu_{avg}	average Nusselt number.
P	pressure, Pa
q''	heat flux, W/m^2
R	radius of the passage, m
Re	Reynolds number, $\rho U D_h/\mu$

T	temperature, K
U	velocity, m/s
x	x-axis, m
X	dimensionless x-axis, x/d
s	dimensional length along the curved surface, m
S	non-dimensional length along the curved surface, s/d

Greek symbols

μ	dynamic viscosity, $kg/m.s$
θ	dimensionless temperature, T/T_{in}
ρ	density, kg/m^3

Subscripts and superscript

avg	averaged value
f	fluid
in	inlet
LM	logarithmic mean
out	outlet